DESIGN OF A GAMMA-RAY SOURCE BASED ON INVERSE COMPTON SCATTERING AT THE FAST SUPERCONDUCTING LINAC*

D. Mihalcea[1], B. Jacobson[2], A. Murokh[2], P. Piot[1,3], and J. Ruan[3]
[1] Department of Physics and Northern Illinois Center for Accelerator & Detector Development, Northern Illinois University DeKalb, IL 60115, USA
[2] Radiabeam Technologies, Santa Monica, CA 90404, USA
[3] Fermi National Accelerator Laboratory, Batavia IL 60510, USA

Abstract

A watt-level average-power gamma-ray source is currently under development at the Fermilab Accelerator Science & Technology (FAST) facility. The source is based on the Inverse Compton Scattering of a high-brightness 300-MeV beam against a high-power laser beam circulating in an optical cavity. The back scattered gamma rays are expected to have photon energies up to 1.5 MeV. This paper discusses the optimization of the source, its performances, and the main challenges ahead.

INTRODUCTION

The range of x- and γ-ray applications, already impressive, could increase even further pending the availability of small-footprint sources. High dose, high brightness and monochromatic x-rays can be generated via synchrotron radiation at large accelerator facilities which are extensively used for fundamental scientific research. More compact sources could have a large variety of applications for national defense industry and medicine. The most promising process which can be at the base of future compact x- and γ-ray is the Inverse Compton Scattering (ICS) [1,2]. Essentially, ICS consists of head-on collision between an electron beam and a laser. The energy of the scattered photons [3] is much higher than of the incident photons because of a double-Doppler frequency upshift:

$$\omega_s = \frac{4\gamma^2}{1 + \frac{a_0^2}{2} + \gamma^2\theta^2}\omega_L, \tag{1}$$

where ω_s and ω_L are the frequencies of the scattered radiation and of the laser respectively, γ the relativistic factor of the electron beam, a_0 the normalized vector potential ($a_0 \equiv \frac{eA}{mc}$) and θ the observation angle with respect to the electron beam. Although ICS also needs an electron accelerator, the $\propto \gamma^2$ dependence of the scattered photon energies makes this technique promising because only a small to medium size accelerator is needed. For example, at FAST the electron energy reaches about 300 MeV and after the collision with infrared laser pulses ($\hbar\omega_L \simeq 1.2$ eV) the scattered photon energy is $\hbar\omega_L \leq 1.5$ MeV.

The other γ-ray source properties can be similar to those produced at large electron facilities. At FAST we expect that each single electron pulse to produce a γ-ray pulse with brightness in excess of 10^{20} photons/[s-(mm-mrad)^2-0.1%BW]. In normal operation FAST linac delivers trains of about 3,000 pulses each second. Under some approximations [4] valid for most experimental conditions including those at FAST the γ-ray brightness can be expressed in terms of laser and electron beam parameters:

$$B_x \propto \frac{N_\gamma}{\sigma_L^2}\gamma^2\frac{N_e}{\Delta t_e \epsilon_{n,x}^2}, \tag{2}$$

where N_γ is the number of photons in the laser pulse, σ_L is the laser transverse size (rms), γ electron beam relativistic factor, N_e number of electrons in the bunch, Δt_e electron pulse length and $\epsilon_{n,x}$ electron beam normalized transverse emittance. At FAST γ and Δt_e are fixed at about 600 and 3 ps rms respectively.

Under similar approximations [4] the scattered photon dose depends on the laser and electron beam properties as

$$N_x \approx \frac{N_e N_\gamma \sigma_T}{2\pi(\sigma_e^2 + \sigma_L^2)}, \tag{3}$$

where N_e, N_γ, σ_L have the same meaning as in Eq. (2), σ_T is the total Thompson scattering cross section and σ_e is the electron beam transverse size (rms).

The monochromaticity of the scattered beam, more often referred as bandwidth is defined as the relative energy spread of the scattered photons in the observation direction. In practice bandwidth is heavily dominated by the electron beam angular spread [3]:

$$BW(\%) \approx \frac{\epsilon_{n,x}^2}{\sigma_e^2} \tag{4}$$

In the next section we describe some of the experimental challenges. The following section contains results of simulations aimed to optimize the performances of the scattered radiation and the last section contains the conclusions.

EXPERIMENTAL CHALLENGES

The laser beam used for ICS experiment originates from the IR laser system used to extract the electrons from the photocathode after conversion to UV (266 nm). The IR-to-UV conversion efficiency is small (~ 10%) so that most

* This work was sponsored by the DNDO award 2015-DN-077-ARI094 to Northern Illinois University. Fermilab is operated by Fermi Research Alliance, LLC. for the U.S. Department of Energy under contract DE-AC02-07CH11359.

ISBN 978-3-95450-169-4

of the IR is available for further use. Our approach is to condition and amplified the IR pulse using two single-pass amplifiers to bring the laser pulse energy from about 50 µJ to about 50 mJ eventually. To further increase the pulse energy to Joule level we plan to use a passive enhancement cavity. This type of cavities were intensively studied in the recent years and intensity amplification factors of several thousands were obtained [5, 6]. An amplified IR laser pulses enter in such a cavity, illustrated in Fig. 1, from the left side and undergo an integer number of round trips, a new laser pulse arrives at the cavity entrance. Assuming a optimal mode matching the amplitude of the two pulses add up coherently. The intensity increase is limited only by the loses in the mirrors [7]. The process is repeated with the subsequent IR pulse. Once the steady state is reached the pulse intensity in the cavity is

$$I = \frac{1 - R_1}{1 - \sqrt{(R_1 R_2)^n}} I_L \tag{5}$$

where R_1 and R_2 are the reflectivities of the two mirrors, n is the number of roundtrips performed by the laser pulse inside the cavity during the time interval between consecutive bunches coming from the laser system and I_L is the intensity of the laser pulses just before the entrance in the cavity. As an example, for commercially-available mirrors

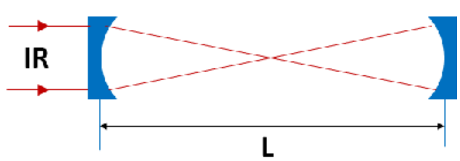

Figure 1: Schematic representation of a Fabry-Perot cavity consisting of two concave mirrors to enhance the IR pulses coming from the left side of the mirrors.

with $R_1 = 0.999$, $R_2 = 0.99995$ and $n = 1$ the amplification factor is $\frac{I}{I_L} \approx 3,626$. It is important to note that the "entrance" mirror, in this example R_1, must have a much lower reflectivity in order to allow the outside laser pulses to couple to the cavity. Also, to diminish the loses inside the cavity, it is convenient that the number of roundtrips is kept to minimum $n = 1$. This latest condition is not always easy to fulfill. For example, in our case the laser sampling frequency is 3 MHz which makes the distance between consecutive pulses 100 m. To maintain the cavity length to a reasonable value of about $L = 2$ m requires $n = 25$. With the same mirrors the decrease of the amplification factor is dramatic $\frac{I}{I_L} \approx 6$. A more sophisticated cavity design in addition perhaps to an increased laser frequency is currently being explored.

The interaction point between the electrons and the laser pulses will occur inside the enhancement cavity ideally where the transverse size of the laser beam reaches a minimum. The laser waist w_0 determines the transverse size of the laser beam at mirrors $w(z) = w_0\sqrt{1 + \left(\frac{z}{z_R}\right)^2}$ where Rayleigh length z_R is defined as $z_R \equiv \frac{\pi w_0^2}{\lambda_L}$. Assuming for example that $z = 1$ m and the radius of the laser spot at mirrors should not exceed 1 cm then the laser beam waist is constrained: $w_0 > 30$ µm and consequently $z_R > 2.7$ mm. Obviously, this constraint will depend on the final enhancement cavity design.

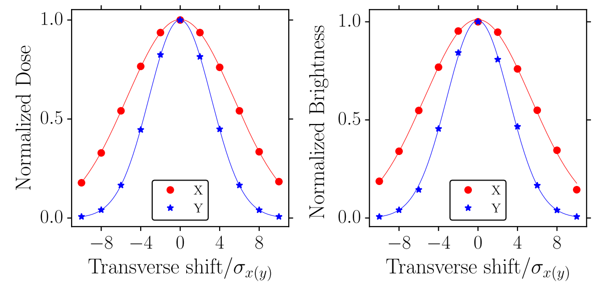

Figure 2: Scattered radiation dose (left) and peak brightness (right) as functions of trajectory displacement in transverse plane. The displacements are in units of electron bunch sigma's and radiation parameters are normalized to maximum values when there are no displacements.

Since both electron and laser beams transverse sizes are expected to be of the order of 10 µm small misalignment of the two beams may cause significant decrease of the critical scattered beam parameters: dose and brightness. As Fig. 2 shows displacement of about $4\sigma_x$ in x-direction could cause a decrease of the main parameters of about 30 %. The situation is even worse in the y-direction (assumed here to be the direction of the laser polarization) where the same displacement could cause more 50 % signal reduction. The longitudinal synchronization is also very important because the scattered radiation dose and brightness are both $\propto \frac{1}{w_0^2}$ and a delay between the two beams of about $\frac{z_R}{c} \approx 1$ ps would decrease the two parameters by a factor of 2. The solution found at Radiabeam is to use photoconductive THz antenna in order to longitudinally synchronize the two beams [8].

GAMMA-RAY PARAMETER OPTIMIZATION

The simulation code described in Ref. [3] was used to tune the electron and laser beam parameters such that scattered beam brightness, dose and bandwidth are optimized. This code allows the analysis of spatial, temporal and spectral properties of the scattered γ-rays for a specific combination of electron and laser beam input parameters. Although the code can deal with the ICS non-linear effects, parameterized by the normalized vector potential a_0 in Eq. (1), the laser intensity determined by laser pulse energy (0.5 J) and beam waist ($w_0 = 30$ µm) is low enough ($a_0^2 = 0.0076$) to make the results insensitive to whether these effects are included or not in the simulations.

Our previous beam dynamics studies [9] show that the transverse normalized emittance is correlated with the electron bunch charge: $Q(nC) \approx 0.34\epsilon_{nx}^{1.45}$ (µm). Instead of this relationship we assume a more conservatine linear corre-

ISBN 978-3-95450-169-4

lation $Q(nC) \approx 3 \times \epsilon_{n,x}$ which approximates well the the previous equation when electron bunch charge is in the range 100 pC to 3 nC. This empirical relationship makes the combination of dose N_x and brightness B_x, $A_x \equiv N_x \times B_x \propto \frac{1}{\sigma_e^2+\sigma_L^2}$ to depend exclusively on beams transverse size.

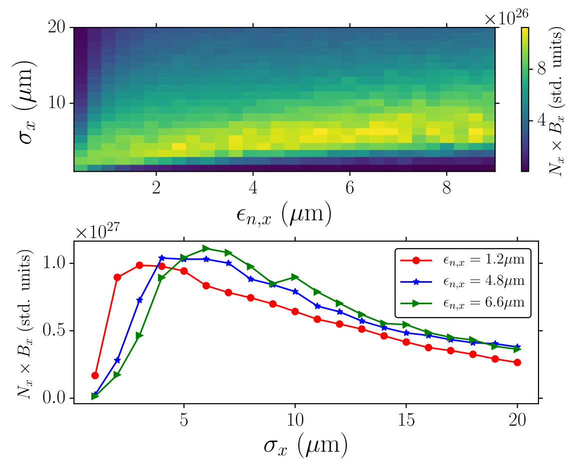

Figure 3: Top plot: scatter plot of the product $N_x \times B_x$ as a function of electron beam transverse emittance and transverse size. Bottom plot: $N_x \times B_x$ as a function of electron beam transverse size for different values of the emittance.

In these simulations only first 1% most energetic scattered photons are retained and scans are performed in the two-dimensional space determined by electron beam transverse emittance and transverse size. The laser waist is fixed at 30 µ. The value of A_x, Fig. 3 is relatively constant with respect to emittance and, as expected, decreases at large transverse size σ_x. At very low transverse electron beam size (<3 µm), A_x unexpectedly decreases but in this region the scaling relations described by Eqs. (2) and (3) are not valid. By inspecting Fig. 3 electron beam transverse size $\sigma_x = 5$ µm maximizes A_x over a large range of electron beam transverse emittance. Also, to keep the bandwidth from Eq. (4) close to about 2 % the emittance should be about 0.6 µm. Finally, according to the empirical relationship mentioned above, the electron bunch charge is about 200 pC.

In practice only a small fraction of the most energetic photons are used. Collimators can be used to select these photons because the angular spread is smaller for higher energy photons (Eq. (1)). In Table 1 the most important scattered beam parameters are shown when top 1 %, 3 % and 100 % of generated photons are taken into consideration. As expected, peak brightness and bandwidth are better when only a small fraction of most energetic photons are retained. The dose decreases for smaller subsamples almost linearly.

CONCLUSIONS

The electron beam parameters at FAST critical for this experiment are: normalized transverse emittance of a few microns when bunch charge is 1 nC, relative energy spread of about 0.1 % and transverse beam size of a few microns at 300 MeV beam energy. The duration of the klystron pulse is about 1 ms and the laser sampling rate is 3 MHz. Therefore, trains of about 3,000 electron bunches can be generated at FAST.

Table 1: Optimized γ-ray Parameters for Different Energy Filters; see text for details.

Energy filter	1 %	3 %	100 %
Brightness (std. units)	2.7×10^{20}	2.1×10^{20}	1.1×10^{20}
Dose (photons)	5.4×10^5	2.0×10^6	4.8×10^7
Bandwidth (%)	0.25	0.82	2.2

Since the brightness and dose of the scattered radiation are proportional with the laser pulse energy, the design and manufacturing of the laser enhancement cavity are crucial for this project's success. An amplification factor of at least 100 and laser beam waist at interaction point of at most 30 µm are needed. Transverse cavity alignment should be in the micron range and longitudinal synchronization of the order electron bunch duration (3 ps).

The scaling relations for brightness and dose in conjunction with the empirical linear dependence of the electron emittance on bunch charge were used to optimize the main parameters of the scattered radiation. For top 1 % most energetic scattered photons we expect peak brightness in excess of 10^{20} photons/[s-(mm-mrad)^2-0.1%BW] dose of the order of 10^5-10^6 photons/pulse and bandwidth below 1 %. These values correspond to a single electron pulse. Brightness and dose should be multiplied by the number of bunches available within 1 sec ($\approx 15,000$) for nominal operation with 1-ms the RF macropulse repeated at 5 Hz.

REFERENCES

[1] F. Arutyunyan and V. Tumanyan, *Sov. J. Exp. Theor, Phys.*, **17**, 1417, (1963).

[2] O. Kulikov, Y. Telnov, and M. Yakimenko, *Phys. Lett.*, **13**, 344, (1964).

[3] W. J. Brown and F. V. Hartemann, *Phys. Rev. ST Accel. Beams*, **7**, 060703, (2004).

[4] W. J. Brown and F. V. Hartemann, *AIP Conference Proceedings*, **737**, 839, (2004).

[5] H. Shimizu, A. Aryshev, Y. Higashi, Y. Honda, and J. Urakawa, *NIM* A, **745**, 63-72, (2014).

[6] V. Brisson, *et al.*, *NIM* A, **608**, 575-577, (2009).

[7] P. Haar, I. M. Fishman, T. I. Smith, and H. A. Schwettman, *NIM* A, **318**, 899-902, (1992).

[8] B. Jacobson, Fermilab IOTA Workshop, June 15, (2016).

[9] P. Piot, Y. -E. Sun, and M. Church, in *Proc. IPAC'10*, Kyoto, Japan, (2010).

ISBN 978-3-95450-169-4